ACTA MECHANICA SINICA (English Series), Vol.12, No.1, Feb. 1996 ISSN 0567-7718
The Chinese Society of Theoretical and Applied Mechanics
Chinese Journal of Mechanics Press, Beijing, China
Allerton Press, INC., New York, U.S.A.

MOLECULAR DYNAMICS STUDIES ON THE DISLOCATION GLIDING NEAR A TILT BOUNDARY *

Chen Zhiying (陈致英)
(*Institute of Mechanics, Academia Sinica, Beijing* 100080, *China*)

ABSTRACT: The gliding behavior of edge dislocation near a grain boundary(GB) in copper under pure shear stresses is simulated by using molecular dynamics(MD) method. Many-body potential incorporating the embedded atom method (EAM) is used. The critical shear stresses for a single disocation to pass across GB surface are obtained at values of σ_c=23MPa $\sim$ 68 MPa and 137 MPa$\sim$274 MPa for Σ=165 small angle tilt GB at 300 K and 20 K, respectively. The first result agrees with the experimental yield stress σ_y(=42 MPa) quite well. It suggests that there might be one of the reasons of initial plastic yielding caused by single dislocation gliding across GB. In addition, there might be possibility to obtain yield strength from microscopic analysis. Moreover, the experimental value of σ_y at low temperature is generally higher than that at room temperature. So, these results are in conformity qualitatively with experimental fact. On the other hand, the Σ=25 GB is too strong an obstacle to the dislocation. In this case, a dislocation is able to pass across GB under relatively low stress only when it is driven by other dislocations. This is taken to mean that dislocation pile-up must be built up in front of this kind of GB, if this GB may take effect on the process of plastic deformation.

KEY WORDS: molecular dynamics, grain boundary, dislocation, copper, yielding

1 INTRODUCTION

It is well-known that the yield stress of metals is dependent upon grain size as shown by Hall-Petch relation[1]:

$$\sigma_y = ad^{1/2} \tag{1}$$

where σ_y is the yield stress, d is the grain diameter and a is a material constant. Equation (1) shows the importance of grain boundary(GB) in relation to plastic deformation. From the microscopic point of view, plastic deformation of polycrystalline metals is related to the sliding of lattice dislocations across GB and/or other interfaces. Therefore, dislocation-GB interaction plays an important role in understanding microscopically the mechanical properties of metals, which were reviewed by many authors[2,3].

Molecular dynamics (MD) method is useful in revealing the conditions and mechanisms of dislocation gliding near a GB. It was found for example that the lattice dislocation is

Received 30 June 1995, revised 8 November 1995
* The project supported by KM85-33 of Academia Sinica and the National Natural Science Foundation of China

shown to be absorbed by Σ=9 GB and dissociates into GB dislocations in a study on crack propagation in iron using MD method[4]. It is in agreement with the description based upon observations using electron microscopy[5]. In this article, we emphasize only one point: under what conditions lattice dislocations will pass through grain boundaries when external stresses are exerted. The effects of external load, GB structure and temperature upon this phenomenon are investigated.

In MD studies, the treatment of border conditions is difficult when the computational cell is not characterized by periodicity. In this work, a mixed border condition is employed for an asymmetrical cell. Moreover, a many-body inter-atomic potential using embedded atom method(EAM) for copper is used. The computational model and method of calculation are described in II, the main results and discussions are given in III and the conclusions are given in IV.

2 DESCRIPTION OF THE MODEL AND METHOD OF COMPUTATION

2.1 Computational Cell

Because of the complexity of dislocation gliding behavior near GB, it is too difficult to describe it with a relatively small number of atoms in computer simulation. Therefore, a rather simple model is chosen, in which the dislocation line is parallel to GB surface, so that the interaction phenomena can be investigated in a two-dimensional model. It enables the slip transfer across GB because the two slip planes of both crystals and the GB surface have a common intersection line[6]. In addition, the slip planes and the slip directions of the incoming and transmitted dislocations are in small misorientation, so that, such a model ensures that the dislocation is able to pass across GB in an easy way.

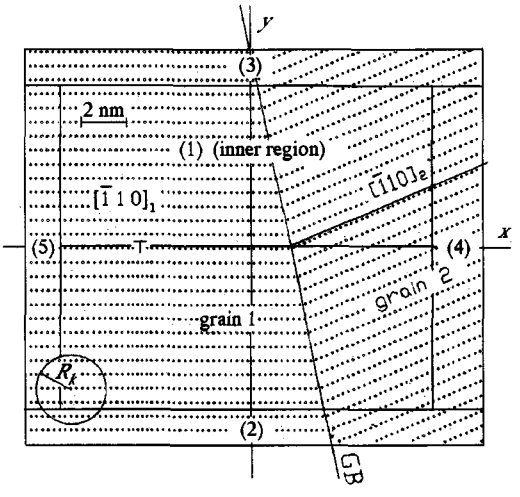

Fig.1 Initial computational cell (Σ=25, 13 522 atoms)

Based upon the above considerations, a thin rectangular cell is chosen, which contains either about 13 500 atoms(at 20 K) or about 27 000 atoms(at 300 K). A coincidence site lattice (CSL) tilt boundary with turning axis $[\bar{1}\bar{1}2]$ is located at about the central part of the computational cell (Fig.1). The coordinate axes are set to be X-$[\bar{1}10]$, Y-$[\bar{1}\bar{1}\bar{1}]$ and Z-$[\bar{1}\bar{1}2]$ of grain 1. An edge dislocation of $(111)/[\bar{1}10]$ is initially preset in grain 1 with

Burgers' vector $b = \frac{1}{2}[\bar{1}10]$. Two different GB structures are considered. One is Σ=165 $(\overline{10}8\bar{1})/[\bar{1}12]15.50°$ and the other is Σ=25$(\overline{7}5\bar{1})/[\bar{1}\bar{1}2]$ 156.93°. The normals to GB surfaces are oriented at 7.75° and 11.54° with respect to the X-axis for the Σ=165 and Σ=25 GB, so that the slip directions $[\bar{1}10]$ of the two grains differ by 15.5° and 23.07°, respectively.

2.2 Equations and Units

The EAM potential of copper is represented by the following formulas[7]: The potential energy of atom i is written as

$$U_i = -f(\rho_i) + \frac{1}{2}\sum_{j\neq i}^{N} V_{ij} \tag{2}$$

where V_{ij} is a central pair potential function, $f(\rho_i)$ is an embedding function which takes the form of a square root function and

$$\rho_i = \sum_{j\neq i}^{N} \phi_{ij} \tag{3}$$

V_{ij} and ϕ_{ij} are functions of inter-atomic distance r_{ij}, which are written as

$$V_{ij} = \sum_{k=1}^{6} a_k (r_k - r_{ij})^3 H(r_k - r_{ij}) \tag{4}$$

$$\phi_{ij} = \sum_{k=1}^{2} A_k (R_k - r_{ij})^3 H(R_k - r_{ij}) \tag{5}$$

respectively, where r_k and R_k are chosen as knot points such that $r_1 > r_2 > r_3 > r_4 > r_5 > r_6$ and $R_1 > R_2$. $H(x) = 0$ for $x < 0$ and $H(x) = 1$ for $x > 0$. Hence, $r_1(= R_1)$ represents the cutoff distance R_c of V_{ij} and ϕ_{ij}. The potential energy of the system is

$$U = \sum_{i=1}^{N} U_i = -\sum_{i=1}^{N} f(\rho_i) + \frac{1}{2}\sum_{i=1}^{N}\sum_{j\neq i}^{N} V_{ij} \tag{6}$$

and the force exerting on atom i is

$$\boldsymbol{F}_i = -\mathrm{grad}_i(U) \tag{7}$$

From Eqs.(1)~(6), we get

$$\boldsymbol{F}_i = -\sum_{j\neq i}^{N} \left[V'(r_{ij}) - \frac{1}{2}\left(\frac{1}{\sqrt{\rho_i}} + \frac{1}{\sqrt{\rho_j}}\right)\phi'(r_{ij})\right]\frac{\boldsymbol{r}_{ij}}{r_{ij}} \tag{8}$$

where $V'(r_{ij})$ and $\phi'(r_{ij})$ are derivatives with respect to r_{ij}. The equation of motion of atom i is

$$m\frac{\mathrm{d}^2\boldsymbol{r}_i}{\mathrm{d}t^2} = \boldsymbol{F}_i \tag{9}$$

which can be solved with given initial conditions by using central difference method[8]. The system of units has been chosen to be:

[energy] — 1 eV(=1.60207×10^{-19} J),

[length] — crystal constant corresponding to the given temperature, which is 3.607 4 $\times$ 10^{-10} m at room temperature,

[mass] — atomic mass of copper =$1.054\,658\times10^{-25}$ kg.

The crystal constants at different temperatures are calculated with the standard value at 293.16 K and the coefficient of linear thermal expansion α=1.7×10^{-5} K^{-1}. From these fundamental units, other units can be derived:

[time] — $2.913\,318\times10^{-13}$ s,

[velocity] — $1.232\,494\times10^{3}$ m/s,

[force] — $4.440\,550\times10^{-10}$ N.

Thus, all of the calculations are performed in terms of dimensionless quantities and equations.

2.3 Border and Initial Conditions

In general, for periodic border conditions it is required that the size of the computational cell Δl should be chosen to be at least twice the cutoff distance R_c of the potential function. If this is satisfied, it is quite easy for an atom to find its neighbors within a sphere of radius R_c. In this case, only one nearest image of the atom of main cell needs to be taken into account. If $\Delta l < 2R_c$, at least two atomic images have to be considered. Likewise, if $\Delta l < R_c$, four or more atomic images need to be considered. In the present model, the lattice structure in Z direction has a natural period containing six atomic layers. Thus, periodic border condition can be used reasonably. To save computer time, we would rather use the least thickness in Z direction Δl_z. Therefore, we take such a natural period as the thickness of the cell in the case of low temperature (20 K). The length of such a period is only Δl_z = 4.397 6 Å(1Å= 10^{-10} m) at 20 K (the effective Δl_z will reduce to 4.363 1Åafter solid translation). In this case, four nearest atomic images should be considered, because Δl_z is smaller than the cutoff distance $R_c(R_c = r_c = 4.418, 1Å)$. However, at 300 K, two natural periods are considered because of larger thermal fluctuation. So, Δl_z is definitely larger than R_c and two atomic images are sufficient for the periodic condition.

The sizes along X and Y directions are chosen to be about 50 and 40 times the crystal constant, respectively. The cell is not periodic in these directions, so that periodic border condition is inapplicable. Moreover, the flexible border condition designed for fitting the elastic strain field of an edge dislocation[9,10] is not convenient due to the movement of dislocation. Therefore, we adopt a mixed border condition for the X and Y borders. This border condition is now explained in detail. The cell is divided into 5 regions in X and Y directions as shown in Fig.1. Region 1 is an inner region, in which atoms move in accordance with Eqn.(9) during atomic relaxation. Regions 2$\sim$5 are outer regions (borders). For regions 3 and 5, fixed border condition is used, whereas for regions 2 and 4, a movable border condition is suggested. As the atomic relaxation process of the inner region takes place, atoms in the movable borders are relaxed with the same displacements as average values of their neighbors of inner region. Such a border relaxation works at each time step. Moreover, the force acting on an atom is affected by the nearby atomic configuration within a sphere centered on this atom with a radius R_k (Fig.1), which is equal to the double cutoff distance R_c of EAM potential, so that the thickness of all the borders must be larger than R_k. Thus, we take the dimensions of the border regions 2, 3 and 5 to be R_k plus a small length. Since the dislocation finally moves out of the right border, a larger size in X direction

of region 4 is considered.

The initial velocities of the atoms in the inner region are randomly given to be in a Maxwellian distribution according to the given temperature T_0.

2.4 Solid Translations

Before atomic relaxation, solid translations between the two grains are performed by shifting grain 2 in X, Y and Z directions until the potential energy reaches its minimum. In the case of $\Sigma 165$ and $\Sigma 25$, the solid translations result in reductions of grain boundary energy about 0.06 and 1.0 J/m^2, respectively.

2.5 Shear Stresses

Two ways of exerting shear stresses to the dislocation are used. The first one is to use fixed border condition on the left border of the cell, so that there will be an effective shear stress σ_e arising from the interaction between the fixed border and the dislocation. It is a repulsive shear exerting on the dislocation[11]. The calculation of the exact value of σ_e is rather complicated, but it can be roughly estimated as an repulsive shear stress originated from its mirror image as shown in Fig.2. Thus, from dislocation theory, σ_e is easily found, which decreases with the increase of the distance Δx between the dislocation center and the left border. It reduces to σ_0=137 MPa when the dislocation reaches GB surface. (Young's modulus of Cu is taken from Handbook of Chemistry and Physics, 37th editioin. The Poisson's ratio of brass is used as 0.37 approximately.) The second way is to give an additional shear strain ϵ of the whole cell by giving every atom an X displacement proportional to its Y coordinate. The additional shear stress σ_1 originated from the shear strain can be estimated by linear elasticity theory. Sometimes, both ways have been used simultaneously, i.e. the total stress exerting on the dislocation is σ_a=σ_e+ σ_1. It is a pure shear stress along $[\bar{1}10]$ in the slip plane (111) of grain 1.

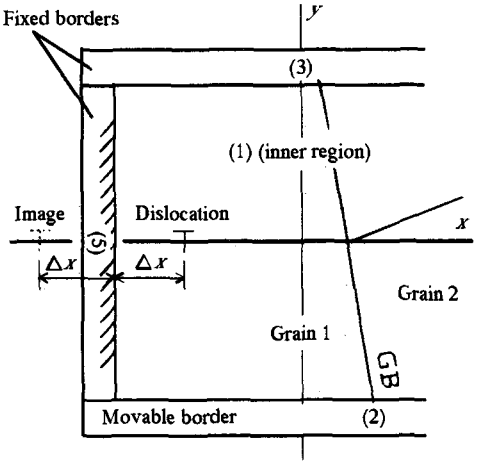

Fig.2 Dislocation and its image

2.6 Relaxation

After solid translations, relaxation of the atomic configuration in the inner region is performed by solving Eq. (9) with the central difference method. The time step is usually chosen to be 0.01. The temperature is kept constant during atomic relaxation by using a "heating" procedure[12] in which the atomic velocities are adjusted according to the average temperature in a short time interval, e.g. 10 time steps. By this procedure, the average temperature is kept nearly constant with an error of about $\pm 1\%$.

The atomic configurations are obtained after each time step. Since the temporary atomic positions fluctuate due to the atomic vibration, in order to get an approximately stationary atomic configuration, the positions of atoms are averaged over 50~100 time steps. From these average configurations, the dislocation gliding behavior near GB is displayed quite clearly.

3 RESULTS AND DISCUSSIONS

3.1 GB as an Obstacle to the Dislocation Gliding

A single edge dislocation gliding process approaching a Σ=25 CSL tilt GB is simulated at T = 20 K under shear stress from the mirror image. The number of atoms is 135 22. Figs.3(a)~(f) show the 100 time-step averaged atomic configurations at different time t when the dislocation glides from its initial position(about 95Å apart from GB) to GB. It can be seen from Fig.3(a)~(d) that the dislocation center approaches GB surface closer and closer, and reaches it at t = 20.0 as shown in Fig.3(d). Thereafter, it fluctuates near GB surface with a distance of about 2~3 crystal constants as displayed by Fig.3(e)~(f). It shows that the dislocation is unable to pass through Σ25 GB under σ_a=σ_0=137 MPa and grain 2 is not disturbed. Fig.4 gives the time evolution of the positions of dislocation core (1) in the presence of GB, and (2) without GB surface (3). From these curves, it is clear that Σ25 GB serves as an obstacle to single edge dislocation under σ_a=137 MPa at 20 K and does not have significant migration.

Curve (3) shows the dislocation gliding process without GB. The coincidence of curve (1) with (3) before t = 18 indicates that GB surface does not give important effect to the dislocation gliding until it is very close to GB. It confirms that GB produces a short range stress field, which agrees with the analysis in the literature[1].

3.2 The Effect of Shear Stress

Increasing the shear stress gradually, one can see how large a local shear stress is sufficient for the single dislocation to pass across a GB. The runs are carried out for Σ=25 GB at 20K under different shear stresses. The stress varies from 274 MPa to 685 MPa. Curves(1)~(4) of Fig.5 give the time evolution of dislocation gliding, which correspond to the shear stresses σ_a=274 MPa, 342 MPa, 411 MPa, and 685 MPa, respectively. Curve(5) shows the GB migration process in the case of 274 MPa, which is not significantly affected by the value of shear stresses. From Fig.5, it is seen that the dislocation is prevented by GB under σ_a=342 MPa, but it can pass across GB under large stresses. From curves (2) and (3), it is concluded that the critical stress σ_c lies between 342 MPa and 411 MPa.

In Fig.5, the coincidence of the portion of curves (1)~(4) before t = 18 gives another evidence that GB surface produces a short range stress field.

3.3 The Effect of Different GB Structures

In order to test the dislocation gliding behavior affected by different GB structures, the following runs are carried out for a Σ=165 CSL tilt GB at 20 K. The number of atoms is 134 76. σ_a takes the values of 137 MPa, 274 MPa, 533 MPa and 930 MPa, respectively. Fig.6 gives the results under different stresses with curves (1)~(4). From these curves, it is seen that the general picture of the dislocation gliding is similar to that of Σ=25, except that the critical shear stress σ_c is lower, which lies between 137 MPa and 274 MPa as indicated by curves (1) and (2).

Comparing curve(2) of Fig.6 and curve (1) of Fig.5, it is seen that the dislocation is able to pass across Σ=165 GB but not across Σ=25 GB under the same shear stress σ_a=274MPa. It shows that Σ25 GB is a stronger obstacle to dislocation gliding than the Σ165 GB. That is to say, Σ25 GB produces a stronger stress field. It is due to its shorter CSL period and higher GB energy[13]

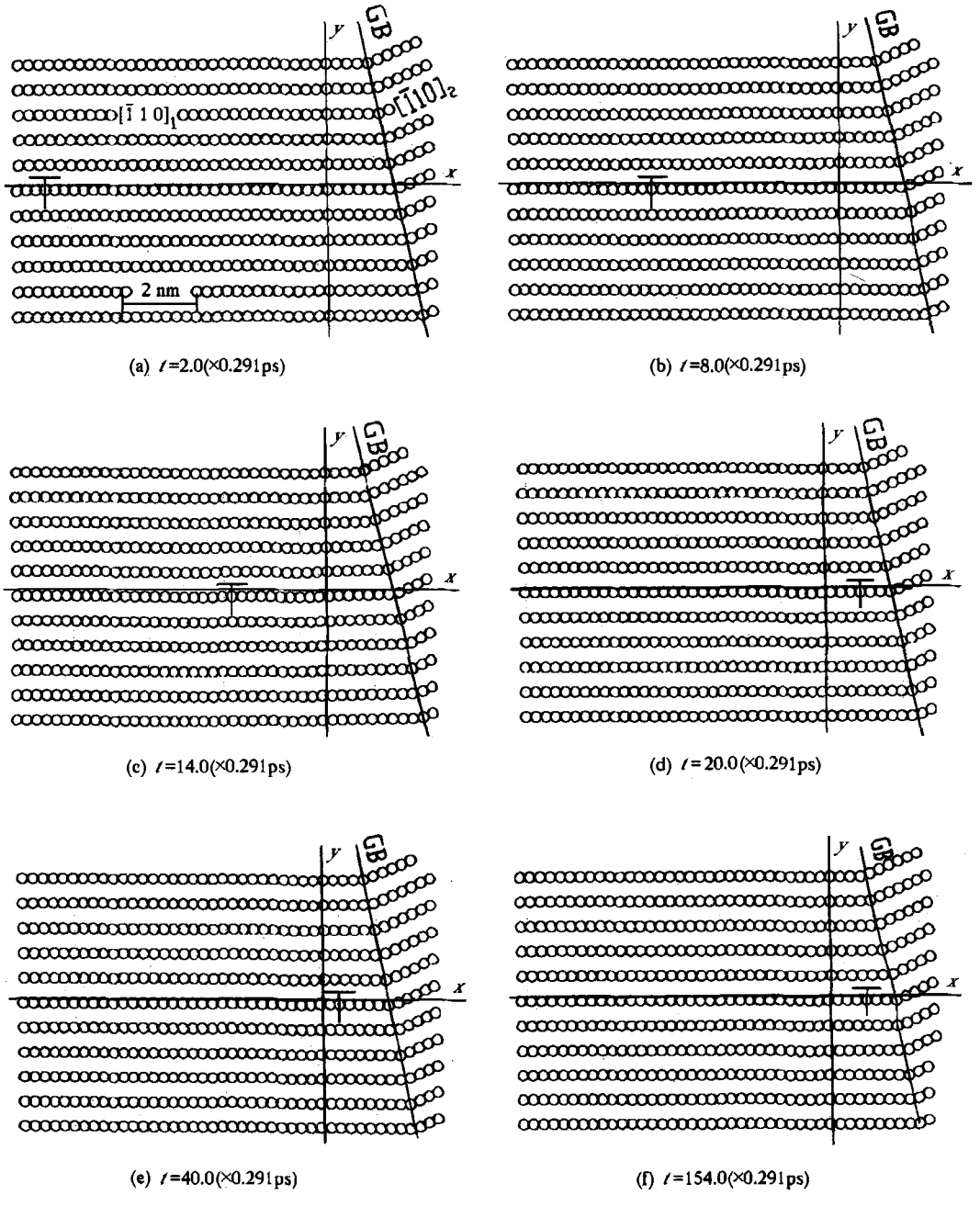

(a) t=2.0(×0.291ps) (b) t=8.0(×0.291ps)

(c) t=14.0(×0.291ps) (d) t=20.0(×0.291ps)

(e) t=40.0(×0.291ps) (f) t=154.0(×0.291ps)

Fig.3 Atomic configurations at different times
($\Sigma = 25, T = 20$ K, 135 22 atoms)
(shear stress σ_a=137 MPa)

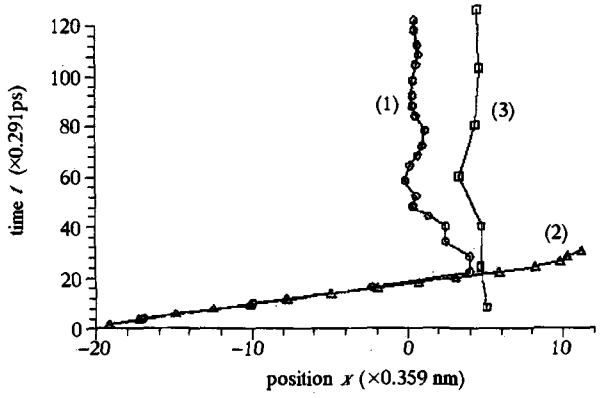

Fig.4 Dislocation gliding processes (1) in the presence of GB, and (2) without GB
($\Sigma = 25, T = 20\,\mathrm{K}$, 13 522 atoms)

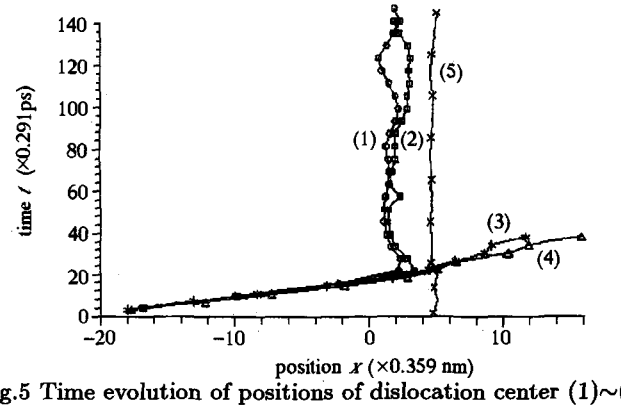

Fig.5 Time evolution of positions of dislocation center (1)~(4)
and GB surface (5) under different shear stresses
($\Sigma = 25, T = 20\,\mathrm{K}$, 13 522 atoms)
(1) $\sigma_a = 274\,\mathrm{MPa}$, (2) $\sigma_a = 342\,\mathrm{MPa}$, (3) $\sigma_a = 411\mathrm{MPa}$, (4) $\sigma_a = 685\,\mathrm{MPa}$

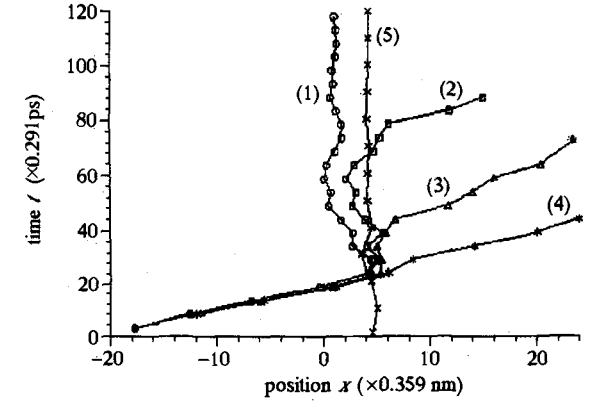

Fig.6 Time evolution of positions of dislocation center (1)~(4) and
GB surface (5) under different shear stresses
($\Sigma = 165, T = 20\,\mathrm{K}$, 13 476 atoms)
(1) $\sigma_a = 137\,\mathrm{MPa}$, (2) $\sigma_a = 274\,\mathrm{MPa}$, (3) $\sigma_a = 533\,\mathrm{MPa}$, (4) $\sigma_a = 930\,\mathrm{MPa}$

3.4 Temperature Effect

The above simulations are all performed at 20 K. It is known that at low temperature the yield stress is higher than that at room temperature. It is because the dislocation glides across GB more difficultly at low temperature. In order to check if the critical shear stress is lower at room temperature than that at 20 K, a series of runs are carried out at 300 K. Because of large thermal fluctuation of atomic movement, the MD simulation at 300 K is rather complicated. In this case, a thicker computational cell is used which has a thickness of two natural periods along Z direction ($L_z = 8.795$Å$= 2.44949$ times the crystal constant) and includes 26952 atoms. The results are shown by curves (1)~(5) in Fig.7, which correspond to the shear stresses σ_a =23, 68, 137, 930 and 1720 MPa, respectively. Curve (6) shows the GB migration process in the case of 137 MPa, which is not significantly affected by the value of shear stress, similar to the case of $\Sigma 25$ and 20 K. From curves (1)~(5) of Fig.7, it is seen that the dislocation can pass across GB under large stresses, but it is prevented by GB under σ_a=23 MPa. From curves (1) and (2), we conclude that the critical shear stress σ_c lies between 23 MPa and 68 MPa.

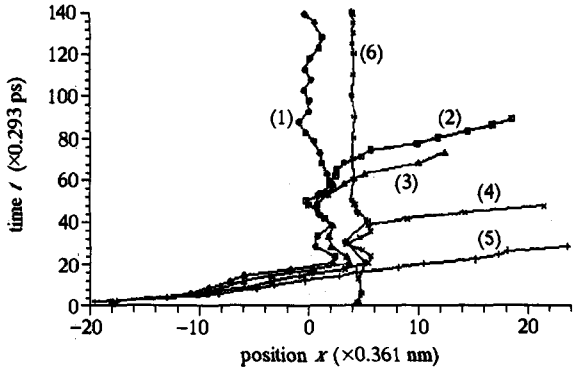

Fig.7 Time evolution of positions of dislocation centers (1)~(5) and GB surface (6) under different shear stresses ($\Sigma = 165, T = 300$ K, 26 952 atoms)
(1) $\sigma_a = 23$ MPa, (2) $\sigma_a = 68$ MPa, (3) $\sigma_a = 137$ MPa, (4) $\sigma_a = 930$ MPa, (5) $\sigma_a = 1\,720$ MPa

It is interesting that the experimental yield stress of copper σ_y is 42 MPa[14]. Therefore, the simulated critical stress of $\Sigma 165$ at 300 K agrees with σ_y quite well. In a polycrystalline material there must be a lot of different GB. Therefore, when yielding starts, it must be some dislocations in easiest conditions to pass across some GB and result in yielding. The above agreement shows that $\Sigma 165$ appears to be one of such GB. It suggests that one of the reasons of the initial plastic yielding might be the single dislocation gliding across some GB in the easiest slip planes and the easiest slip directions. In addition, it appears that there exists possibility to obtain the yield strength of metals based upon the microscopic computer simulations. Any way, this is only a preliminary point of view and needs further studies, because the results are rather limited.

Fig.8 shows the experimental yield shear stress and the simulated critical shear stress vs. temperature. As indicated above, at 300 K the simulated σ_c agrees with the experimental data quite well, but the experimental data spread only to $T = 100$ K, so that we can not

compare the simulated result at 20 K with the measured one directly. Nevertheless, the experimental yield stresses increase with the reduction of temperature and the simulated data are in conformity with the experimental fact qualitatively.

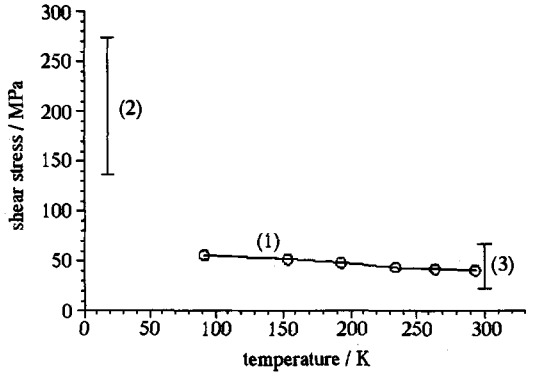

Fig.8 Experimental yield stresses and simulated critical stresses
(1) experimental (Ref.[14], p.20) (2),(3) simulated (this work)

3.5 Two or More Dislocations

As the results described in §3.3 show, $\Sigma 25$ GB is a stronger obstacle to the gliding of a single dislocation. It seems that $\Sigma 25$ GB can not make contribution to the initial yielding. However, it is well known that dislocation pile-up plays important role to dislocation sliding in facing an obstacle like GB. A much larger local shear stress is exerted on the leading dislocation of dislocation pile-up even when the external shear stress is small. Actually, the leading dislocation is driven by subsequent dislocations, so that it glides more easily across GB surface than the single one does. Thus, $\Sigma 25$ GB may also make contribution to the initial yielding, if there is dislocation pile-up in front of it. The simulation of gliding process of one dislocation driven by other dislocations is helpful for revealing the gliding behavior of the leading dislocation in a dislocation pile-up. Thus, a simulation is carried out, in which a second dislocation is added while the first one is close to GB, and then, a third one is added again while the second one is close to GB. By this procedure, it is hoped to simulate what happens when dislocation is driven by others just like the situation in a dislocation pile-up. $\Sigma 25$ GB is used at $T = 20$ K under shear stress by mirror images. Time evolution of the positions of first dislocation, second dislocation, third dislocation and GB is shown in Fig.9. Curve (1) shows the behavior of first dislocation without pushing of other dislocations. In fact, it is similar to curve (1) in Fig.5. Curve (2) of Fig.9 shows that the first dislocation starts to pass through GB after the second one has been added at $t = 30$. Thereafter, the second one glides as curve(3) and is also prevented by GB after $t = 50$. It starts to pass across GB when the third one is added at $t = 65$. Curve(4) shows the gliding process of the second dislocation pushed by the third one. Finally, the third dislocation glides as curve (5) and is also prevented by GB after $t = 95$.

In this simulation, while the second dislocation has not been added, the shear stress exerting on the first one is σ_e, which originates from the mirror image of the dislocation and becomes 137 MPa when it approches GB. As shown by Fig.5, the critical stress σ_c is over 342 MPa, so that, it is certainly unable to pass across GB. However, after the second dislocation has been added, the stress exerted on the first one increases by several times, so that it excesses σ_c. It is the reason why the first dislocation starts to pass through GB at

$t = 30$. But, when it arrives at the right side of GB, the gliding behavior of the second one on the left side has the same feature as that of the first one before $t = 30$. Thus, the second dislocation is still prevented by GB. So does the third dislocation.

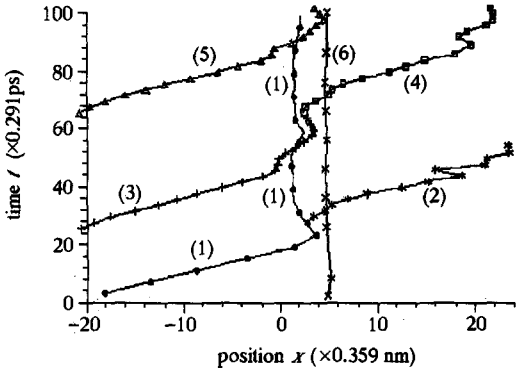

Fig.9 Time evolution of positions of dislocation centers
while they are added one after another
(Σ165, 20 K, 137 MPa, 13 476 atoms)
(1) 1st dislocation only, (2) 1st dislocation after 2nd one added,
(3) 2nd dislocation, (4) 2nd dislacation after 3rd one added, (5) 3rd dislocation

The phenomenon in the above simulation is not the same as that of a dislocation pile-up. In a dislocation pile-up, there exist a lot of dislocations simultaneously. It can not be simulated by so small a computational cell. However, the simulated phenomenon is similar to the dislocation pile-up in one point: the first dislocation is driven by others. Therefore, this work just shows that for some strong obstacle(GB) the sliding of dislocations across GB might happen in dislocation pile-up.

4. CONCLUSIONS

The above results can be summarized into the following conclusions:

(1) MD shows that GB produces a short range stress field and serves as an obstacle to the dislocation gliding. A single edge dislocation in the easiest slip plane and the easiest slip direction is able to pass across some CSL tilt GB, while the local shear stress excesses a critical value.

(2) At 300 K, the critical shear stress σ_c lies between 23 MPa and 68 MPa for Σ=165$(\bar{1}08\bar{1})$ / $[\bar{1}\bar{1}2]$15.50° CSL GB. It coincides with the experimental yield stress σ_y(=42 MPa) quite well. It suggests that the initial plastic yielding might be caused by the single dislocation gliding across some GB as one of the reasons. In addition, it appears that there exists a possibility to obtain yield strength of metals based on the microscopic analysis, even though it needs further studies.

(3) The value of σ_c for Σ=165 at 20 K lies between 137 MPa and 274 MPa, which is higher than that at 300K. That is to say, σ_c increases with the temperature reducing, which is in conformity with the experimental fact qualitatively.

(4) For Σ=25$(\bar{7}5\bar{1})/[\bar{1}\bar{1}2]$156.93° CSL GB, the value of critical shear stress σ_c of a single dislocation is between 342 MPa and 411 MPa at 20 K. But, when the dislocation is followed by other dislocations, it passes across GB quite easily. It is similar to what happens

in the case of a dislocation pile-up. It suggests that for some strong obstacle (GB), the sliding of dislocations across GB during initial yielding might happen in dislocation pile-up.

Acknowledgment: The author would like to acknowledge Profs.Zheng ZM, Cui JP, Ding JQ and Hong YS for the valuable comments and discussions, and also Miss. Wei MZ and Mr. Yuan Q for the programming and data processing.

REFERENCES

1 Hirth JP, Lothe J. Theory of Dislocations. New York: Wiley, 1982: 788, 733
2 Hirth JP. The influence of grain boundaries on mechanical properties. *Metall Trans*, 1972, 3(12): 3047~3067
3 Reed-Hill RE. Physical Metallurgy Principles. New Jersey: Van Nostrand, 1973: 228
4 Ishita Y, Mori M, Hashimoto M. Molecular dynamical calculation of crack propagation in segregeted grain boundaries of iron. *Surface Science*, 1984, 144: 253~266
5 Shen Z, Wagoner RH, Clark WAT. Dislocation and grain boandary interactions in metals. *Acta Metall*, 1988, 36(12): 3231~3242
6 Sittner P, Pal-Val PP, Paidar V. Strength of Metals and Alloys. Edited by Kettunen, PO, Lepisto TK & Lehtonen ME, (Oxford: Pergamon), 1988, 1:427
7 Ackland GJ, Tichy G, Vitek V, Finnis MW. Simple N-body polentials for the noble metals and nickel. *Phil Mag A*, 1987, 56(6): 735~756
8 Cotterill RMJ, Leffers T, Lilholt H. A molecular dynamics approach to grain boundary structure and nugration. *Phil Mag*, 1974, 30(2): 265~275
9 Sinclair JE. Improved atomistic model of a bcc dislocation core. *J. Appl. Phys.*, 1971, 42(13): 5321~5329
10 Hoagland RG, Hirth JP, Gehlen PC. Atomic simulation of the dislocation core structure and Peierls stress in alkali halide. *Phil Mag*, 1976, 34(3): 413~439
11 Dundurs J. Mathematical Theory of Dislocations. edited by Mura T, New York: American society of Mechanical Engineering, 1969: 70
12 Chen ZY, Ding JQ, Tsai DH. Molecular dynamical study of the energy relaxation processes after heating the vibrational degree of freedom in a diatomic molecalar crystal. *Acta Mechanica Sinica*, 1988, 4(4): 372~377
13 Zhang YZ. Theory of Dislocation. Wu Han: Press of Huazhong Institute of Technology, 1988: 183 (in Chinese)
14 Yan MG. (chief editor). Practical Handbook on Engineering Materials. Beijing: Chinese Standard Press, 1989, 4:20 (in Chinese)